Evidence for Interaction between Transmembrane Segments in Assembly of Kv1.3[†]

ZuFang Sheng,[‡] William Skach,[§] Vincent Santarelli,[||] and Carol Deutsch*,[‡]

Department of Physiology and Department of Molecular and Cellular Engineering, University of Pennsylvania, Philadelphia, Pennsylvania 19104-6085, and Department of Physiology, Jefferson Medical College, Philadelphia, Pennsylvania 19107

Received June 23, 1997; Revised Manuscript Received October 2, 1997[⊗]

ABSTRACT: Previously, we showed that the N-terminal recognition domain (T1) of Kv1.3 was not required for assembly of functional channels [Tu et al. (1996) *J. Biol. Chem. 271*, 18904−18911]. Moreover, specific Kv1.3 peptide fragments including regions of the central core are able to inhibit expression of current produced from a channel lacking the T1 domain, Kv1.3(T1$^-$). To elucidate the mechanism whereby Kv1.3 peptide fragments suppress Kv1.3(T1$^-$) current, we have studied the ability of peptide fragments containing the transmembrane segments S1, S1-S2, or S1-S2-S3 to physically associate with the Kv1.3(T1$^-$) polypeptide subunit *in vitro* in microsomal membranes. Using c-myc (9E10) epitope-labeled peptide fragments and anti-myc antibody as well as antisera to the Kv1.3 C-terminus, we now demonstrate specific association of these peptide fragments with Kv1.3(T1$^-$). Association of peptide fragments with Kv1.3(T1$^-$) was correlated with integration of both proteins into the membrane. Furthermore, the relative strength and kinetics of this association directly correlated with the ability of fragments to suppress Kv1.3(T1$^-$) current. The rate-limiting step in the sequential synthesis, integration, and formation of a complex was the association of integrated polypeptides within the plane of the lipid bilayer. These results strongly suggest that the physical association of transmembrane segments provides the basis for suppression of K^+ channel function by K^+ channel peptide fragments *in vivo*. Moreover, the S1-S2-S3 peptide fragment potently suppressed full-length Kv1.3, thus implicating a role for the S1-S2-S3 region of Kv1.3 in the assembly of the Kv1.3 channel. We refer to these putative association sites as IMA (intramembrane association) sites.

Most ion channels are oligomers with wide-ranging homo- and heteromultimeric stoichiometries. Voltage-gated K^+ channels are homotetrameric, and each subunit contains six putative transmembrane segments, S1−S6. The channel subunits are not linked covalently, which is true of many oligomeric membrane proteins (*1*), yet dissociation constants of $<10^{-8}$ are typical for multimers, which means that free energies of dissociation are >10 kcal per interface (*2*). So, what kinds of interactions provide the energy to hold these subunits together? Hydrogen bonds, ion pairs, helix dipole interactions, and lipid packing effects are candidates (*3*). In some cases, the NH_2-terminal domains of ion channels function as recognition motifs (*4*−*7*), but it is not clear that elements of specific recognition between subunits contribute to stabilization of the mature multimeric protein or whether additional subunit−subunit interactions between transmembrane segments provide the energy to shift the equilibrium in a lipid bilayer toward multimerization. Moreover, interactions between transmembrane segments may be highly specific, e.g., the dimerization of glycophorin A (*8, 9*), assembly of the class II major histocompatibility complex (*10*), and of the T-cell antigen receptor (*11, 12*). In the first two examples, close packing of complementary helical interfaces defines the specificity, whereas in the latter case, ion-pair formation is thought to be involved.

Kv1.3, a voltage-gated K^+-selective channel found in T lymphocytes (*13, 14*) forms a non-dissociating tetramer in the lymphocyte plasma membrane (*15*). Assembly of this channel likely involves multiple interactions between different parts of the protein, including the cytoplasmic amino-terminus, which is known to contain a recognition domain for tetramerization (T1) (*5, 6, 16, 17*). However, Kv1.3(T1$^-$), a deletion mutant of Kv1.3 that lacks the first 141 amino acids, produces currents in oocytes with properties identical to those produced by full-length Kv1.3 (*18*). We have interpreted this finding to mean that there are association sites in the central core of Kv1.3 that provide sufficient stabilization interactions for channel assembly and that disruption of one or more of these interactions may cause suppression of channel formation. Co-expression of a variety of peptide fragments containing transmembrane segments from the hydrophobic core of Kv1.3 along with Kv1.3(T1$^-$) results in various levels of expressed current (*18*). These fragments fall into three categories: those that suppressed strongly, those that suppressed at intermediate levels, and those that did not suppress. Examples of these fragments include S1-S2-S3, S1-S2, and S1, respectively. Co-translation of truncated peptide fragments with Kv1.3(T1$^-$) neither prevented translation of Kv1.3(T1$^-$) nor increased its rate of degradation (*18*).

To understand how these peptides effect suppression, we have studied the *in vitro* association of S1, S1-S2, and S1-S2-S3 with Kv1.3(T1$^-$) in a rabbit reticulocyte translation system supplemented with microsomal membranes, a system known to generate fully functional *Shaker* K^+ channels (*19*). We now demonstrate that Kv1.3 peptide fragments physically associate with Kv1.3(T1$^-$), that this association is specific

[†] Supported by National Institutes of Health Grants GM52302 and GM53457.

[‡] Department of Physiology, University of Pennsylvania.

[§] Department of Molecular and Cellular Engineering, University of Pennsylvania.

[||] Department of Physiology, Jefferson Medical College.

[⊗] Abstract published in *Advance ACS Abstracts,* November 15, 1997.

S0006-2960(97)01490-6 CCC: $14.00

and is correlated with efficient integration of peptide fragments and Kv1.3(T1$^-$) into the same membrane, that the strength and the kinetics of association are greater for strong suppressors than for non-suppressors, and that synthesis and integration of K^+ channel protein occur quickly and are not the rate-limiting steps in the formation of an associated complex. Our results strongly suggest that the mechanism of suppression of K^+ channel function by transmembrane peptide fragments is due to direct physical association of the peptide fragment with K^+ channel protein and provide evidence for intramembrane association (IMA) sites in tetramer stabilization.

MATERIALS AND METHODS

Oocyte Expression and Electrophysiology. Oocytes were isolated from *Xenopus laevis* females (Xenopus I, Michigan) as described previously (*20*). Stage V−VI oocytes were selected and micro-injected with 10 ng of cRNA encoding for Kv1.3(T1$^-$), 0.2 ng for Kv1.3 full-length, or 8 ng for Kv3.1, respectively. The mole ratio of cRNA injected for Kv1.3, Kv1.3(T1$^-$), or Kv3.1 channel genes to truncated K^+ channel gene or transmembrane control gene (mouse CD4) was 1:2. K^+ currents from cRNA-injected oocytes were measured with two-microelectrode voltage clamp using a TEC 01C oocyte clamp (NPI Electronic Gmbh, Tamm, Germany) after 24−48 h, at which time currents were 2−10 μA. This level of expressed current was optimal for observing suppression. Electrodes (<1 MW) contained 3 M KCl. The bath Ringer solution contained (in mM) the following: 116 NaCl, 2 KCl, 1.8 $CaCl_2$, 2 $MgCl_2$, and 5 Hepes (pH 7.6). The holding potential was −100 mV. Data are presented as box plots, which represent the central tendency of the measured current. The box and the bars indicate 25−75 and 10−90 percentile of the data, respectively. The horizontal line inside each box represents the median of the data. To determine steady-state inactivation, we recorded from oocytes held for 2.5 s at voltages from −100 to −10 mV (10-mV steps), then at −100 mV for 0.1 ms, and finally to a test voltage of +50 mV for 45 ms. Between stimuli, the oocytes were held at −100 mV for 50 s.

Recombinant DNA Techniques. Standard methods of plasmid DNA preparation, restriction enzyme analysis, agarose gel electrophoresis, and bacterial transformation were used. All isolated fragments were purified with "Geneclean" (Bio 101 Inc., La Jolla, CA), re-circularized using T4 DNA ligase, and then used to transform DH5α or XL1-blue competent cells (BRL, Inc., Gaithersburg, MD). The nucleotide sequences at the 5′ ends of all NH_2-terminal deletion mutants and at the 3′ ends of all C-terminal deletion mutants were confirmed by restriction enzyme analysis or by DNA sequence analysis (Sequenase Version 2.0 DNA sequencing Kit, USB, Inc., Cleveland, OH).

Plasmid Constructs. Clone pSP/Kv1.3(T1$^-$) was generated by cutting pSP vector with *Nco*I/*Xba*I, cutting pGEM/Kv1.3 (*21*) with *Nco*I/*Spe*I, and ligating the vector and the insert. Clone pSP/myc-Kv1.3(T1$^-$) was generated by ligating an oligonucleotide linker encoding the c-myc epitope (MEQKLISEEDL) at the initial *Nco*I site (ATG start codon) of the plasmid pSP/Kv1.3(T1$^-$). Clones pSP/myc-S1, pSP/myc-S1-S2, and pSP/myc-S1-S2-S3 were generated by using pSP/myc Kv1.3(T1$^-$) as a template, a sense oligonucleotide starting at SP6, and the antisense oligonucleotides for S1, S1-S2, and S1-S2-S3, respectively (antisense oligos were GGAGCTGGATCCCTACGTCGAGGCGGGGTAG for S1, GGAGCTGGATCCCTACGAGAAGGTGGCTTTGC for S1-S2, and GGAGCTGGATCCCTAAGACATGGCCTGCTG for S1-S2-S3). Clones of pSP/S1-S2-S3 were generated by using pSP/Kv1.3(T1$^-$) as a template, a sense oligonucleotide starting at SP6, and the antisense oligonucleotide for S1-S2-S3. Plasmids S.L.ST.gG.P and BPI, which encode a transmembrane chimeric protein and a full-length bovine pre-prolactin, respectively, were made as described previously (*22*). Coronavirus (pT7/IBV M; *23*) was given to us by Dr. Carolyn Mackamer (Johns Hopkins University). pRc/CMV/CD4 was derived from XpUC/L3T4 (mouse CD4) given to us by Dr. Jane Parnes (Stanford University). CD4 was isolated by *Eco*RI/*Xba*I digestion and triple ligated with an *Eco*RI/*Pvu*I-digested fragment and an *Xba*I/*Pvu*I-digested fragment, each of which was previously isolated from pRc/CMV. pRc/CMV/rat Kv3.1 was given to us by Dr. Teresa Perney (Yale University).

In Vitro Translation. Capped cRNA was synthesized *in vitro* from linearized templates using Sp6 or T7 RNA polymerase (Promega, Madison, WI). Proteins were translated *in vitro* with [^{35}S]methionine (2 μL/25 μL translation mixture; ∼10 μCi/μL Dupont/NEN Research Products, Boston, MA) for 60−120 min at 30 °C in rabbit reticulocyte lysate, in the presence (1.8 μL membrane suspension/ 25 μL translation mixture) or absence of canine pancreatic microsomal membranes (Promega, Madison, WI or MBI Fermentas, Amherst, NY), according to the Promega Protocol and Application Guide. For co-translation we used an cRNA mole ratio of peptide fragment to protein of 2:1. Microsomal membranes were titrated with cRNA to give maximal co-immunoprecipitation. These concentrations were typically 0.2−0.5 μg cRNA (NH_2Ac-precipitated) and 1.8 μL membranes in 25 μL translation reaction media.

Gel Electrophoresis and Fluorography. Electrophoresis was performed on C.B.S. Scientific gel apparatus using 10% or 15% SDS−polyacrylamide gels made according to standard Sigma protocols (Sigma Technical Bulletin, MWM-100). Following electrophoresis, gels were stained with Coomassie blue and destained. Gels were soaked in Amplify (Amersham Corp., Arlington Heights, IL) to enhance ^{35}S fluorography, dried, and exposed to Kodak X-AR film at −70 °C. Typical exposure times were <36 h. Quantitation of gels was carried out directly using a Molecular Dynamic PhosphoImager (Sunnyvale, CA).

Deglycosylation. *In vitro* translated protein (∼8 μL of translation mixture) was denatured in a total volume of 10 μL containing 1% SDS, 100 mM NaAc (pH 4.5−6), and 50 mM EDTA by heating to 100 °C for 3 min. The reaction was then cooled on ice. A 4-fold excess of NP-40 was added to the reaction to complex the SDS. The reaction volume was increased to 96 μL by addition of a solution containing 50 mM EDTA, 100 mM NaAc, and 1% β-mercaptoethanol, then 4 μL of endoglycosidase F (Boehringer Mannheim, Germany) was added, and the reaction was incubated in a water bath at 37 °C for 4 h. After incubation, 100 μL of SDS−PAGE sample buffer was added.

Immunoprecipitation. One to five microliters of cell-free translation products was mixed in 400 μL of buffer A (0.1 M NaCl, 0.1 M Tris (pH 8.0), 10 mM EDTA, and 1% Triton X-100) containing 0.1 mM phenylmethanesulfonyl fluoride

(PMSF). Ascites fluid (9E10; 1 μL) or antisera (4 μL) was added, and samples were incubated at 4 °C for 30 min. The Kv1.3 antisera was made to the C-terminal epitope, EELRKARSNSTLSKSE in rabbits (Cocalico Biologicals Inc., Reamstown, PA); the anti-c-myc ascites fluid was made to EQKLISEEDL (*24*) by injecting $3-5 \times 10^6$ 9E10 hybridoma cell (ATCC) intraperitoneally into Balb/C mice (Cell Center, University of Pennsylvania). Ascites fluid was centrifuged at 16000*g* for 10 min and stored in aliquots at −70 °C. Protein A Affi-Gel beads (10−20 μL) were added and the suspension mixed continuously at 4 °C for 6−15 h with constant mixing. The beads were centrifuged and washed 3x with Buffer A and 2x with 0.1 M NaCl, 0.1 M Tris (pH 8.0) prior to SDS-PAGE and fluorography. Where relevant, cpm in immunoprecipitated proteins were corrected by the efficiency of recovering precipitated protein from the translation mixture. The correction factor was calculated as the ratio of peptide fragment in the translation mixture to peptide fragment in the immunoprecipitate, as measured using the anti-myc antibody. The efficiency of immunoprecipitation by the c-myc antibody and Kv1.3 antisera ranged from 10−25%. In those cases in which the avidity (strength of association) between peptide fragments and Kv1.3(T1$^-$) was determined by titrating the association with increasing amounts of detergent, sodium dodecyl sulfate (0−1.0% SDS in 0.1M Tris, pH 7.8) or sodium N-dodecanoylsarcosinate (0−0.1% Sarkosyl in 50 mM NaCl, 0.1 M Tris, pH 7.5) was added (100 μL) to the translation products (3.5 μL) and incubated for 30 min at 4 °C before diluting 10× with buffer A (+ PMSF) and continuing according to the procedures described above.

Carbonate Extraction. *In vitro* translation products (1−5 μL) were diluted in 750 μL of either sodium carbonate (0.1 M Na_2CO_3, pH 11.5) or Tris (0.25 M sucrose, 0.1 M Tris, pH 7.5) solution. Samples were incubated on ice for 30 min prior to centrifugation at 70 000 rpm (208 kG) TLA 100.3 rotor for 30 min. Supernatants were removed, and proteins were precipitated in 10% trichloroacetic acid and resuspended in 20 μL of SDS−PAGE sample buffer. Membrane pellets were dissolved directly in SDS−PAGE sample buffer.

RESULTS

To test whether suppression of Kv1.3(T1$^-$) by Kv1.3 peptide fragments involves association of the peptide fragments with Kv1.3(T1$^-$), we used N-terminally tagged peptide fragments (Figure 1A) encoding a c-myc epitope to co-immunoprecipitate Kv1.3(T1$^-$) protein. As shown in Figure 1B, *in vitro* translation of native and myc-tagged Kv1.3 fragments generated protein of the expected size (see legend), with tagged proteins migrating at 1−4 kDa higher molecular masses. There is a single glycosylation site in the loop between S1 and S2 that is absent from the S1 and myc-S1 fragments. Thus, these fragments appear as a single band, whereas S1-S2, S1-S2-S3, and Kv1.3(T1$^-$) each appear as doublets (Figure 1B). Glycosylation was confirmed using Endoglycosidase F digestion (Figure 1C; *18*), and tagged and untagged S1-S2 and S1-S2-S3 were each glycosylated to the same extent. cRNA from each of the tagged and untagged constructs was injected into *Xenopus* oocytes along with cRNA for Kv1.3(T1$^-$), and the resultant current was measured by two-electrode voltage-clamp. Myc-S1 has no effect on Kv1.3(T1$^-$) peak current, as co-injection of Kv1.3(T1$^-$) with S1 and co-injection of Kv1.3(T1$^-$) with myc-S1 gave median currents of 3.83 ± 0.26 μA (n = 9) and 3.77 ± 0.15 μA (n = 9), respectively. These medians are not different (p = 0.86, Mann−Whitney Rank Sum Test), and S1 has been shown previously to have no effect on Kv1.3(T1$^-$) (*18*). However, as shown in Figure 2, myc-S1-S2 and myc-S1-S2-S3 suppressed Kv1.3(T1$^-$) current by 34% (n = 9, p = 0.03) and 68% (n = 9, p = 0.0004), respectively. These results are consistent with our previously reported finding that S1 does not suppress, S1-S2 is an intermediate suppressor, and S1-S2-S3 is a strong suppressor (*18*), indicating that epitope tagging of the NH_2-terminus of each Kv1.3(T1$^-$) fragment does not alter the functional characteristics of the peptide fragments.

These tagged fragments now allowed us to examine whether the suppression of Kv1.3(T1$^-$) currents in oocytes could be mediated by association of peptide with the Kv1.3(T1$^-$) protein. We co-translated truncated Kv1.3(T1$^-$) fragments along with full-length Kv1.3(T1$^-$) in a 2:1 mole ratio of cRNA in a rabbit reticulocyte lysate mixture supplemented with canine pancreatic microsomal membranes. The protein products are shown in Figure 3A along with controls of separately translated Kv1.3(T1$^-$), myc-S1, myc-S1-S2, and myc-S1-S2-S3. Proteins in the translation mixtures were immunoprecipitated using anti-myc antibody and anti-Kv1.3(T1$^-$) antisera directed to the C-terminus of Kv1.3. Figure 3B demonstrates that S1-S2-S3, S1-S2, and S1 fragments were able to co-immunoprecipitate Kv1.3(T1$^-$) polypeptide regardless of whether anti-myc antibody or Kv1.3 antisera was used. The fraction of total Kv1.3(T1$^-$) bound (corrected to the translation mixture) in the presence of myc-S1, myc-S1-S2, and myc-S1−S2-S3, respectively, was 0.067, 0.168, and 0.192 using anti-myc antibody. The fraction of total peptide bound, myc-S1, myc-S1-S2, and myc-S1-S2-S3, respectively, in the presence of Kv1.3(T1$^-$) was 0.003, 0.012, and 0.066 using the Kv1.3(T1$^-$) antisera. These results indicate that association of myc-S1-S2-S3 with Kv1.3(T1$^-$) was 3−20 times more efficient than association of myc-S1. It is unlikely that the less efficient co-immunoprecipitation of Kv1.3(T1$^-$) by myc-S1 is due to self-association of myc-S1 because co-translation of S1 with myc-S1 followed by immunoprecipitation with myc antibody did not produce a S1:myc-S1 complex (data not shown). Both S1-S2-S3 and myc-S1-S2-S3 co-immunoprecipitated equally well with Kv1.3(T1$^-$) using Kv1.3 antisera (data not shown), indicating that association was not altered by the myc epitope.

The association of Kv1.3(T1$^-$) with Kv1.3 peptide fragments appeared to be specific, as demonstrated by the following experiment in which non-K^+ channel proteins were co-translated with Kv1.3(T1$^-$). The control proteins were CD4 (MW = 51 kDa) and IBV M (coronavirus, MW = 25 kDa), which contain one and three transmembrane segments, respectively (*23*). Each of these proteins was translated together with Kv1.3(T1$^-$) in a 2:1 mole ratio, followed by incubation with Kv1.3 antisera and protein A. Figure 4A shows the co-translated products along with controls of separately translated proteins. CD4 has no glycosylation sites and appears as a single band at ∼51 kDa whereas IBV M has two glycosylation sites and the major one of three bands is at 32 kDa. As shown in Figure 4B, neither CD4 nor IBV M co-immunoprecipitated. No bands for these proteins were detected even with exposure times >14 days. The bands at ∼27 kDa in lanes 2, 6, 7, and 8 are background bands derived from Kv1.3(T1$^-$) (lane 2). This experiment indicates that

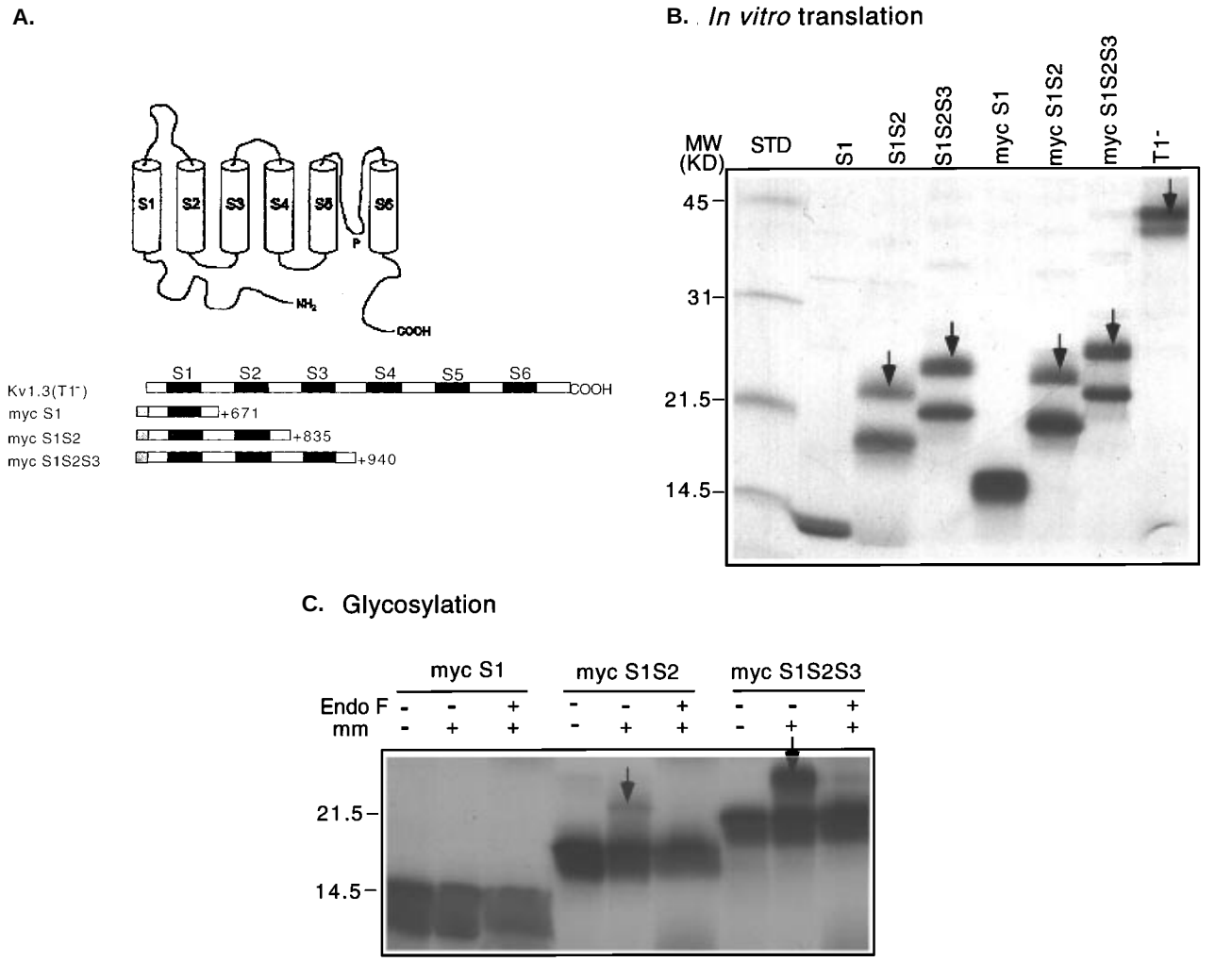

FIGURE 1: *In vitro* translation of Kv1.3(T1$^-$) and peptide fragments. (A) Putative Kv1.3(T1$^-$) subunit topology and schematic drawing of fragments of Kv1.3 cDNA. The solid boxes represent the transmembrane segments, the shaded small box at the NH_2-terminus represents the myc epitope (EQKLISEEDL), and the empty boxes represent the loops between transmembrane segments. The numbers are derived from the full-length, wild-type Kv1.3 clone starting from the ATG start codon (+19) and denote the terminal sites for each construct. The NH_2-terminus for all constructs was +441, i.e., each is an NH_2-terminally deleted fragment. (B) Fluorography of [^{35}S]methionine-labeled peptide fragments without myc or with an N-terminal myc-epitope and Kv1.3(T1$^-$). All proteins were translated in the presence of microsomal membranes and analyzed by SDS−PAGE. S1-S2, S1-S2-S3, and Kv1.3(T1$^-$) each displayed two bands, one that is glycosylated (downward arrows) and one that is unglycosylated. Estimated molecular weights for non-glycosylated bands are 9, 16, 19, and 42 kDa for S1, S1-S2, S1-S2-S3, and Kv1.3(T1$^-$), respectively. (C) Evidence for glycosylation. Myc-labeled peptide fragments were translated and [^{35}S]methionine labeled in the presence (+mm) and absence (−mm) of microsomal membranes. Membrane-asssociated protein was treated with 0.2 unit of endoglycosidase F (endo) for 4 h at 37 °C. For panels B and C, translation was carried out at 30 °C for 60−120 min.

the interactions of myc-labeled S1, S1-S2, and S1-S2-S3 with Kv1.3(T1$^-$) were not simply due to non-specific hydrophobic interactions of *in vitro* co-translated transmembrane proteins.

To explain the differences in association among the peptide fragments, we asked whether the strength of interaction between Kv1.3(T1$^-$) and peptide fragment depended on the nature of the peptide fragment. Ideally, we would like to measure the equilibrium constant for each complex of peptide fragment with Kv1.3(T1$^-$). However, several considerations preclude our determining a true dissociation constant. First, we do not know the precise nature of complex formation. It may be a simple bimolecular reaction of one peptide fragment and one Kv1.3(T1$^-$) to form a dimer complex, or it may be multi-molecular, involving not only peptide fragments and Kv1.3(T1$^-$) in various stoichiometries but also chaperone proteins. Moreover, the association we observe may simply be an aggregation of peptide fragments and Kv1.3(T1$^-$) in a large complex. Second, if association has not reached steady-state, then any measurement of complex formation will reflect an apparent on-rate rather than an equilibrium constant.

To determine the relative strengths of association, we therefore characterized the interaction between each of these peptides and Kv1.3(T1$^-$) using different detergent conditions or varying the concentration of Kv1.3(T1$^-$). First, the fraction of Kv1.3(T1$^-$) bound to peptide fragment was determined for each translation mixture incubated with increasing amounts of either SDS (Figure 5A) or Sarkosyl (Figure 5B). As shown in Figure 5A, the fraction of Kv1.3(T1$^-$) associated with peptide fragment was extremely sensitive to the SDS concentration. The percent of SDS required to dissociate half of the peptide-Kv1.3(T1$^-$) complex was 0.02 and 0.20% for myc-S1 and myc-S1-S2-S3, respectively. The maximum difference in ability of myc-S1 versus myc-S1-S2-S3 to be extracted from membranes at SDS concentrations of 0.05−1.0% is 2-fold (data not shown).

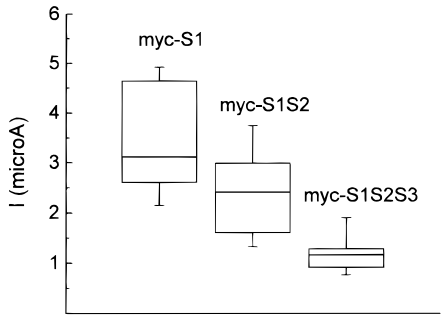

FIGURE 2: Effect of peptide fragments on Kv1.3(T1$^-$) current expressed in oocytes. *Xenopus* oocytes were co-injected with cRNA for Kv1.3(T1$^-$) and either myc-S1, myc-S1-S2, or myc-S1-S2-S3 (in a 1:2 mole ratio), and recordings were made 23 h postinjection. Peak current at +50 mV was measured. Data are represented as box plots ($n = 9$). The median current obtained with myc-S1-S2 and myc-S1-S2-S3 was significantly less than control, with $p = 0.03$ and 0.0004, respectively, as determined from a nonparametric Mann−Whitney rank sum test. The bath Ringer solution contained (in mM): 116 NaCl, 2 KCl, 1.8 $CaCl_2$, 2 $MgCl_2$, 5 Hepes (pH 7.6). The holding potential was −100 mV.

Thus, the 10-fold difference in half-dissociation concentrations reflects a difference of at least 5-fold in avidity for Kv1.3(T1$^-$). These results were not specific to the detergent used. As shown in Figure 5B, at Sarkosyl concentrations that dissociated most of myc-S1 and Kv1.3(T1$^-$), there was little decrease in the fraction of Kv1.3(T1$^-$) bound to myc-S1-S2−S3. Both titrations suggest that myc-S1-S2-S3 associated more strongly with Kv1.3(T1$^-$) than did myc-S1 under the conditions used in the translation reaction. In a similar experiment, myc-S1-S2 exhibited an avidity intermediate between that of myc-S1 and myc-S1-S2-S3 (data not shown). In another approach, we varied the concentration of Kv1.3(T1$^-$) cRNA in the translation reaction while keeping the concentration of the peptide cRNA constant and measured the mole ratio of bound Kv1.3(T1$^-$) to peptide fragment in the translation reaction by co-immunoprecipitation with anti-myc antibody. In this experiment, we used ∼3× greater moles of myc-S1 protein than myc-S1-S2-S3 in order to compensate for the one-third lower efficiency of integration (see below and Table 1). The relative slopes of these plots (10:1 for myc-S1-S2-S3:myc-S1) therefore indicate the relative strengths of interaction of peptide with Kv1.3(T1$^-$). Results from these two different methods both indicate that myc-S1-S2-S3 has a stronger interaction with Kv1.3(T1$^-$) than does myc-S1.

Do these interactions require membranes? If membranes are necessary for the association of peptide fragments with Kv1.3(T1$^-$), then translation of peptide fragments and Kv1.3(T1$^-$) in the absence of microsomal membranes should not produce associated complexes. Figure 6 shows that, when Kv1.3(T1$^-$) was co-translated with myc-labeled peptides in the presence of microsomal membranes, it was immunoprecipitated with anti-myc antibody (Figure 6B, lanes 6, 11, and 16; Figure 6C; also Figure 3). In contrast, in the absence of microsomal membranes, very little Kv1.3(T1$^-$) was immunoprecipitated with anti-myc antibody (Figure 6B, lanes 5, 10, and 15; Figure 6C), demonstrating that association requires the presence of microsomal membranes. [Background bands (Figure 6B: ∼40 kDa, e.g., lanes 8−10, ∼45 kDa, e.g., lanes 8−10 and 13−15) in the vicinity of Kv1.3(T1$^-$) are present and should not be confused with the doublet of Kv1.3(T1$^-$) (arrows)]. In addition, when Kv1.3(T1$^-$) and peptide fragments were translated separately in the presence of membranes and then mixed posttranslationally, no association was observed (Figure 6B, lanes 7, 12, and 17). The fraction of total Kv1.3(T1$^-$) bound to peptide fragment was significant only when Kv1.3(T1$^-$) and peptide fragments were co-translated together in the presence of microsomal membranes (Figure 6C). To further characterize the membrane requirement and temporal sequence for association, we translated peptide fragments separately from Kv1.3(T1$^-$), terminated translation by addition of puromycin, and then mixed the separately translated products together along with microsomal membranes. As shown in Figure 7A, lane c, peptide fragments and Kv1.3(T1$^-$) were not glycosylated. Similarly, when we separately translated peptide fragments in the absence of membranes and Kv1.3(T1$^-$) in the presence of membranes and mixed them together (lanes d), peptide fragments were not glycosylated whereas Kv1.3(T1$^-$) was glycosylated, indicating that the membranes were fully functional. As shown in Figure 7B, for any given peptide, lane b displays relatively large amounts of co-immunoprecipitated Kv1.3(T1$^-$). Neither lane c nor lane d shows evidence for significant immunoprecipitated Kv1.3(T1$^-$). These results are quantified in Figure 7C where the fraction of total Kv1.3(T1$^-$) bound is shown for each translation condition, a−d. For all peptides, bound Kv1.3(T1$^-$) was at least 7−10 times greater when co-translated with peptide in the presence of membranes than when it was either co-translated with peptide in the absence of membranes or separately translated and subsequently mixed with peptide.

Although these results show that membranes are required for association, they do not address whether the peptide fragments must be integrated into the membrane in order to associate with Kv1.3(T1$^-$) and whether, for example, the poorer association of myc-S1 with Kv1.3(T1$^-$) could be due to its inability to integrate into the membrane. Likewise, the greater ability of myc-S1-S2 and myc-S1-S2-S3 to associate with Kv1.3(T1$^-$) may be due to their abilities to integrate better into the membrane. To test this hypothesis, we extracted microsomal membranes with sodium carbonate (pH = 11.5) and compared the results to those obtained with Tris buffer extraction (pH = 7.5). In each case, the extracts were centrifuged to give the pellet and supernatant fractions shown in Figure 8. The following control cRNAs were simultaneously translated: S.L.ST.gG.P, which encodes a chimeric integral membrane protein (45 kDa); BPI, which encodes a secreted full-length bovine pre-prolactin protein (25 kDa) (*22*). The former should remain in the pellet fraction at pH 7.5 and pH 11.5, whereas the latter will be in the pellet (microsome lumen) at pH 7.5 and in the supernatant at pH 11.5. As shown in Figure 8 and Table 1, 89% of total Kv1.3(T1$^-$) translated was integrated into the membrane. Only 29% of total translated myc-S1 was integrated into the membrane, whereas 71% and 90% of myc-S1-S2 and myc-S1-S2-S3, respectively, integrated into the membrane. The fact that these percentages do not achieve 100% is reasonable because the microsomal membranes are limiting in the translation reaction but optimal for co-immunoprecipitation (see Methods). The non-epitope tagged peptide fragments also integrated into microsomal membranes with similar efficiencies (data not shown). These results suggest that the failure of myc-S1 to integrate efficiently into the membrane may also contribute to its inability to suppress Kv1.3(T1$^-$).

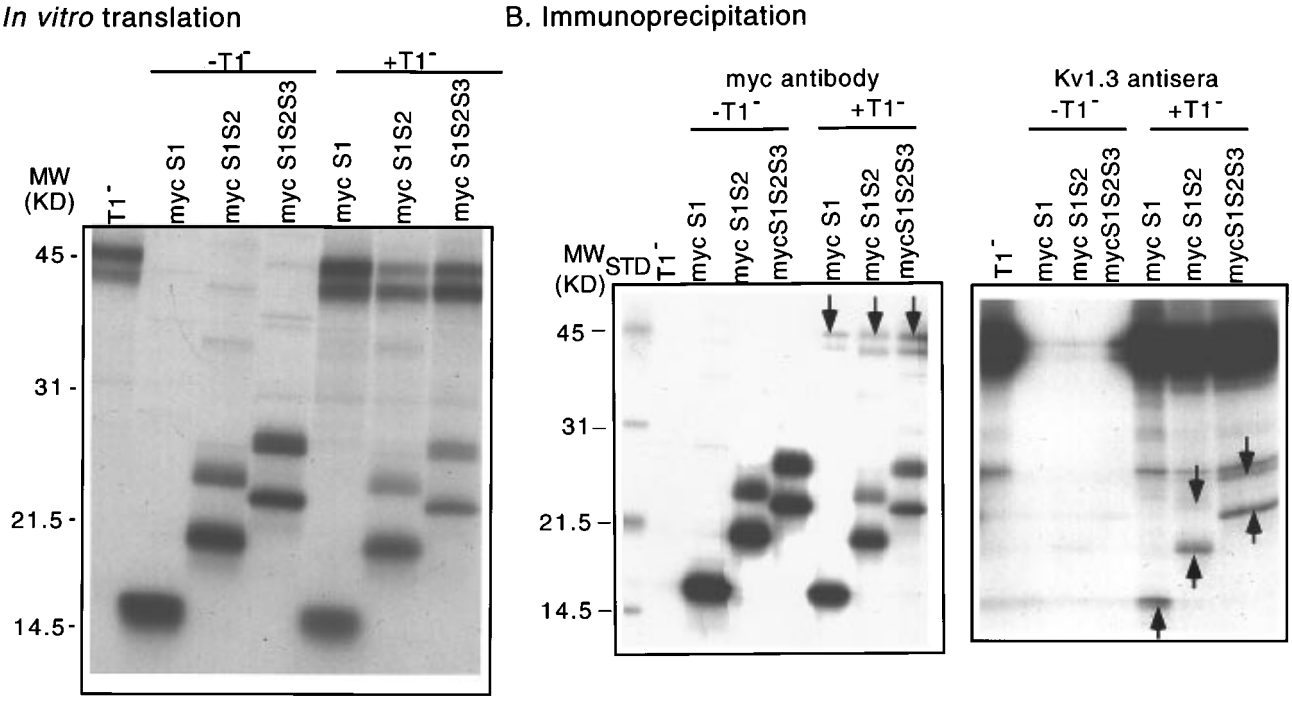

FIGURE 3: Immunoprecipitation of Kv1.3(T1$^-$) with peptide fragments. (A) Kv1.3(T1$^-$), myc-S1, myc-S1-S2, and myc-S1-S2-S3 were each translated separately, or Kv1.3(T1$^-$) was co-translated with myc-S1, myc-S1-S2, or myc-S1-S2-S3 (in a 1:2 mole ratio of cRNA) in the presence of microsomal membranes. (B) The reaction mixture in panel A was immunoprecipitated with an anti-myc antibody or Kv1.3 antisera. Downward arrows in the left panel indicate glycosylation of Kv1.3(T1$^-$), and in the right panel indicate glycosylation of myc-S1-S2 and myc-S1-S2-S3. Upward arrows in the right panel indicate unglycosylated bands of each peptide fragment. The left panel in B shows that anti-myc antibody precipitated Kv1.3(T1$^-$) along with myc-labeled peptide fragments. The right panel shows that Kv1.3 antisera precipitated peptide fragments only when Kv1.3(T1$^-$) was present.

The results shown in Figures 6−8 indicate that association of Kv1.3(T1$^-$) and peptide fragment requires that both chains be synthesized and integrated into the same membrane. If either of these conditions fail to be met, then association is prevented. Consistent with these results, sucrose gradient determinations of monomeric and tetrameric Kv1.3(T1$^-$) translated in the presence or absence of microsomal membranes demonstrate that tetramers form only in the presence of membranes (data not shown). Together these results suggest that interactions responsible for association occur within the plane of the bilayer and directly involve transmembrane segments. To determine whether integration and association are sequential or simultaneous events, we studied the time course of synthesis, integration, and association of Kv1.3(T1$^-$) with peptide fragments. These measurements also addressed whether the different extents of association shown in Figure 5 reflected different association rate constants as well as different apparent avidities. As shown in Figure 9A, synthesis of Kv1.3(T1$^-$) was essentially complete within 30 min. This was true regardless of whether it was translated separately or together with peptide fragments (data not shown). Similarly, synthesis of peptide fragments translated alone or together with Kv1.3(T1$^-$) was also completed within 15−30 min (data not shown), consistent with faster translation of the shorter length fragments. Translation was not limited by the energy source, as addition of creatine phosphate and creatine phosphokinase to the translation mixture did not alter the protein detected (data not shown). Integration of Kv1.3(T1$^-$) and peptide fragments into microsomal membranes was determined concomittantly in parallel samples from the same translation mixture (Figure 9B). Integration of Kv1.3(T1$^-$) into microsomal membranes in the presence of myc-S1 or myc-S1-S2-S3 reached 62−100% of its maximum value within 30 min, consistent with rapid release of chains into the bilayer. Similarly, integration of peptide fragments co-translated with Kv1.3(T1$^-$) reached 100% of its maximum value within 30 min (data not shown). Kinetics and steady-state levels of peptide fragment integration were independent of Kv1.3(T1$^-$). However, Kv1.3(T1$^-$) integration was modified slightly by peptide fragment, equilibrating to a ~22% lower level than in the absence of peptide (data not shown). In contrast, Figure 9C shows that the fraction of total Kv1.3(T1$^-$) associated with myc-S1 and myc-S1-S2-S3 was 4 and 13%, respectively, at 30 min and increased to 31 and 67%, respectively, by 2 h. The absolute percent of bound Kv1.3(T1$^-$) depends on the experimental conditions (e.g., concentration of membranes and of cRNA, hence the difference between data in Figures 7−9). The inset shows that by 2 h the protein mole ratio of Kv1.3(T1$^-$) to myc-S1-S2-S3 was 4.3-fold higher than the mole ratio of Kv1.3(T1$^-$) to myc-S1. For these experiments, the concentration of myc-S1 was twice that of myc-S1-S2-S3. Thus, considering the differences in membrane integration and concentration between myc-S1 and myc-S1-S2-S3, the ratio of the slopes of the inset curves for myc-S1-S2-S3 to that for myc-S1 would be 1.5 if there were no differences in rates of association with Kv1.3(T1$^-$). However, the slope of the curve for moles of T1$^-$/moles of myc-S1-S2-S3 is 4.3 times larger than that for myc-S1, suggesting that there are real differences in rates of association of Kv1.3(T1$^-$) with myc-S1-S2-S3 versus myc-S1. A steady-state level of association was not reached for either myc-S1 or myc-S1-S2-S3 during 2 h of translation. Therefore, the rate constants [i.e., time

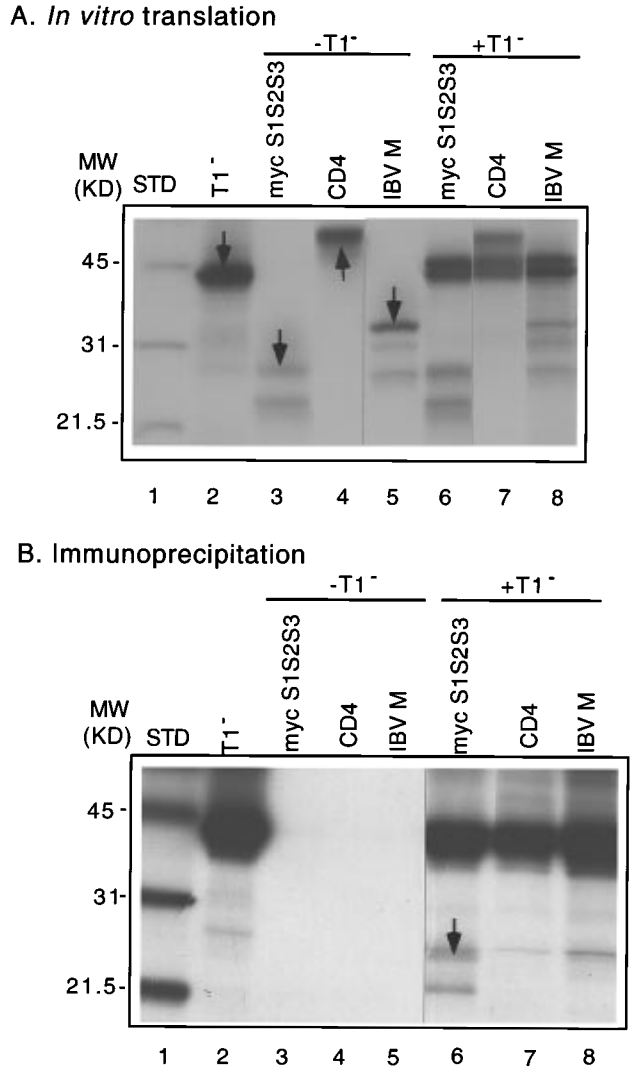

FIGURE 4: Immunoprecipitation of Kv1.3(T1$^-$) with non-channel proteins. (A) Kv1.3(T1$^-$), myc-S1-S2-S3, CD4, and IBV M were each translated alone (lanes 2−5), or myc-S1-S2-S3, CD4, and IBV M were each co-translated with Kv1.3(T1$^-$) in a 2:1 mole ratio with Kv1.3(T1$^-$) (lanes 6−8) in the presence of microsomal membranes. Kv1.3(T1$^-$) appears as a doublet at 42−45 kDa, myc-S1-S2-S3 as a doublet (21−25 kDa), CD4 as a single band at ∼51 kDa, and the major of three bands for IBV M is a glycosylated band at ∼32 kD. (B) The reaction mixtures in panel A were immunoprecipitated with Kv1.3 antisera. Only myc-S1-S2-S3 was co-precipitated. The bands at ∼27 kDa in lanes 2, 6, 7, and 8 are background bands derived from Kv1.3(T1$^-$). Downward arrows indicate glycosylation.

taken to reach (1 − 1/e) of equilibrium level] cannot be determined from these data. However, our results suggest that synthesis and integration of K^+ channel monomers occurs quickly and that the rate-limiting step in formation of an associated monomer:peptide complex is the association step itself in the membrane.

One possible way in which association of myc-S1-S2-S3 with Kv1.3(T1$^-$) could lead to suppression of current would be if this complex were composed of a tetrameric channel plus one or more peptide fragments. Such a complex might have altered channel gating or even altered conductance due to myc-S1-S2-S3 bound to the tetrameric channel. A simple explanation for apparent suppression of K^+ current could be that such a modified channel had shifted voltage-dependent steady-state inactivation so that at +50 mV more channels were inactivated. To test this hypothesis, we determined the steady-state inactivation over a wide range of voltages for Kv1.3(T1$^-$) current expressed in the absence and presence of S1-S2-S3 (suppressed current). As shown in Figure 10, there was no significant difference in the voltage-dependent steady-state inactivation. If anything, the observed small differences (i.e., slight shift of the S1-S2-S3 curve to the right and larger non-inactivating current at positive voltages) would tend to give larger, not smaller Kv1.3(T1$^-$) current in the presence of S1-S2-S3.

Another possible mechanism whereby a tetrameric channel plus one or more peptide fragments could cause suppression of current would be if such a modified channel had a shifted voltage-dependent activation such that the channel opened only at very much more positive voltages. This is highly unlikely because all current measurements were made at +50 mV, and the conductance versus voltage curves for Kv1.3 and Kv1.3(T1$^-$) each saturate at −20 mV (*13*,*18*). Thus, to account for the observed reduced current in the presence of suppressing peptide fragment, a shift of ≥100 mV would be required. This is unprecedented. Theoretically, this could be tested by depolarization to voltages >+100 mV; however, such extreme voltages induce irreversible damage to the oocyte. Moreover, suppressed current shows similar current−voltage curves (data not shown) to that obtained for Kv1.3(T1$^-$) alone. Thus it is unlikely that the residual current observed in the presence of S1-S2-S3 is from channels that contain associated S1-S2-S3. These results are consistent with S1-S2-S3 association with channel subunits to produce non-functional subunits, thereby reducing the population of functional channels.

Although association occurs between the strongly suppressing S1-S2-S3 and Kv1.3(T1$^-$), it is possible that the N-terminal T1 recognition domain contributes significantly to the stabilization energy as well as to subfamily specificity of the full-length Kv1.3 tetramer. If this were true, then the presence of T1 in full-length Kv1.3 might be sufficient to override suppression by S1-S2-S3. We therefore asked whether these fragments could suppress full-length Kv1.3? As shown in Figure 11, when co-injected in a mole ratio of 2:1 (Kv1.3 peptide fragment:Kv1.3 full-length), S1-S2-S3 (derived from Kv1.3) suppressed full-length Kv1.3 by 82%. It also suppressed full-length Kv3.1 by 75%. The average percentage identity and homology between Kv1.3 and Kv3.1 for each of the transmembranes segment in the S1-S2-S3 fragment is 44% and 80%, respectively. S1-S2-S3 derived from Kv1.3 is a potent and promiscuous suppressor of full-length K^+ current expressed by members of at least one other K^+ channel subfamily.

DISCUSSION

Voltage-gated K^+ channels consist of four identical, non-covalently linked subunits (*25*), which upon reaching the plasma membrane do not dissociate (*15*). If this is the case, then what are the interactions that keep this tetramer irreversibly together? Neither the mechanisms nor the interacting surfaces across subunit boundaries are known. It is possible that auxiliary proteins participate in the formation and stabilization of tetramers (*26*), and it is also possible that a tetramer, regardless of the mechanism by which it was formed, is a stable structure in the absence of any auxiliary proteins. The latter possibility is suggested by the work of

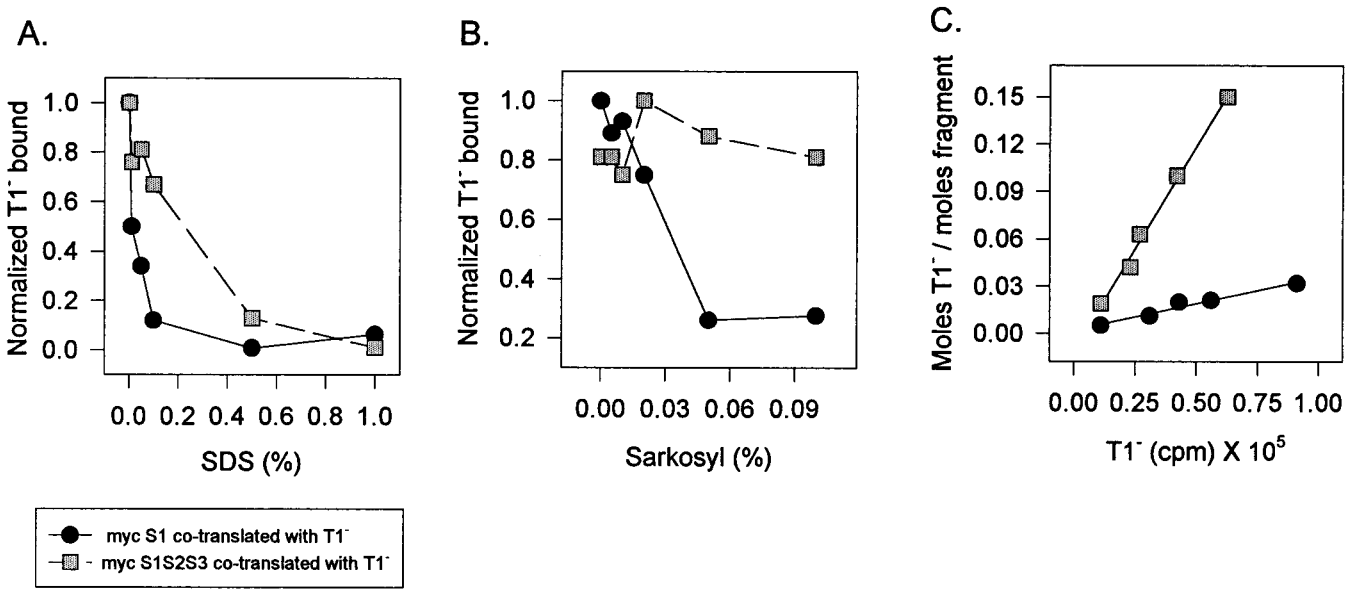

FIGURE 5: Avidity of peptide fragments for Kv1.3(T1$^-$) protein. (A) Kv1.3(T1$^-$) was co-translated with myc-S1 or myc-S1-S2-S3 for 60 min at 30 °C in the presence of microsomal membranes and treated with the indicated concentrations of SDS for 30 min at 4 °C, diluted 10-fold with buffer A, immunoprecipitated with anti-myc antibody as described in Figure 3, and run on SDS−PAGE. The total amount of protein in each translation reaction was approximately equal. The Kv1.3(T1$^-$) bound was normalized to the maximal Kv1.3(T1$^-$) bound for each peptide fragment. (B) Titration was as in panel A, using the indicated concentrations of Sarkosyl. For the data in panels A and B, the maximal fractions of bound Kv1.3(T1$^-$) in the absence of detergent were similar for both myc-S1 and myc-S1-S2-S3 and were 13% for zero SDS and 21% for zero Sarkosyl. (C) Immunoprecipitation of Kv1.3(T1$^-$) and peptide fragments as a function of Kv1.3(T1$^-$) concentration in the *in vitro* translation reaction. Kv1.3(T1$^-$) was co-translated with myc-S1 or myc-S1-S2-S3 at the indicated Kv1.3(T1$^-$) concentrations, immunoprecipitated with anti-myc antibody, as described in Figure 3, and assayed by SDS−PAGE. The total moles of myc-S1 in each translation reaction was 3× the total moles of myc-S1-S2-S3. The ordinate values were calculated as the ratio of bound Kv1.3(T1$^-$) [corrected cpm (see Methods) in the immunoprecipitate] to the total peptide fragment (cpm in the translation mixture). The relative slopes of these plots indicate the relative strengths of interaction of peptide with Kv1.3(T1$^-$). Data shown in panel A are the average of two experiments, and panel B is representative of duplicate experiments.

Table 1: Steady-State Membrane-Associated Fraction[a]

	myc-S1	myc-S1-S2	myc-S1-S2-S3	T1$^-$	TM	BPI	myc-S1 (co-translated with T1$^-$)	myc-S1-S2-S3 (co-translated with T1$^-$)
P/P+S								
pH 7.5	0.5	0.83	0.95	0.94	0.91	0.92	0.36	0.85
pH 11.5	0.29	0.71	0.90	0.89	0.90	0.21	0.24	0.79

[a] P, pellet; S, supernatant. For the data shown in Figure 8, the ratio P/P+S was calculated for extraction at pH 7.5 to give the fraction associated with membranes and for extraction at pH 11.5 to give the fraction integrated into the membranes. The last two columns show ratios calculated for myc-S1 and myc-S1-S2-S3 co-translated with Kv1.3(T1$^-$).

Spencer et al. (*27*), who showed that purified full-length Kv1.3 reconstituted into lipid bilayers forms functional channels with biophysical and pharmacological properties identical to those of native Kv1.3. Moreover, it has recently been shown that a purified putative K^+ channel homologue from *Streptomyces lividans* can form stable homotetramers even in detergent (*28*). Thus, channel proteins themselves can provide sufficient free energy to stabilize tetramers in a membrane environment.

To probe for these putative interaction sites across K^+ channel subunits, our approach has been to test the ability of a series of hydrophobic Kv1.3 peptide fragments to suppress Kv1.3(T1$^-$) current when both are heterologously expressed in *Xenopus* oocytes. While this strategy has been used in both oocytes and mammalian cells to identify multimerization domains in NH_2-terminal segments of ion channels (*4*, *5*, *7*), it has not been used to probe interactions within the hydrophobic core containing transmembrane segments. Other methods using the yeast two-hybrid system (*17*) or peptide−peptide binding assays (*5*−*7*, *16*) have been used to show that K^+ channel subunits, or parts of these subunits, multimerize both *in vitro* and *in vivo*, but again these studies have been concerned primarily with cytoplasmic NH_2-terminal interactions.

Previously we have shown that Kv1.3 peptide fragments fall into three categories: strong suppressors, intermediate suppressors, and non-suppressors (*18*). These peptide fragments do not suppress by enhancing degradation of Kv1.3(T1$^-$) protein *in vivo* (*18*). Because suppressed current is essentially identical to non-suppressed current with respect to biophysical characteristics (see above and ref 18), we have hypothesized that peptide fragments associate with channel subunits to produce non-functional subunits, thereby reducing the population of functional channels. If this is true, then peptide fragments should physically associate with channel subunits. To test this hypothesis, we have chosen to study one peptide fragment from each of these groups, namely, S1, S1-S2, and S1-S2-S3, respectively. Each was modified by appending a c-myc epitope to the NH_2-terminus to allow us to show physical interaction with Kv1.3(T1$^-$).

The peptide fragments associated with Kv1.3(T1$^-$) to different degrees. myc-S1 associated slightly, whereas myc-

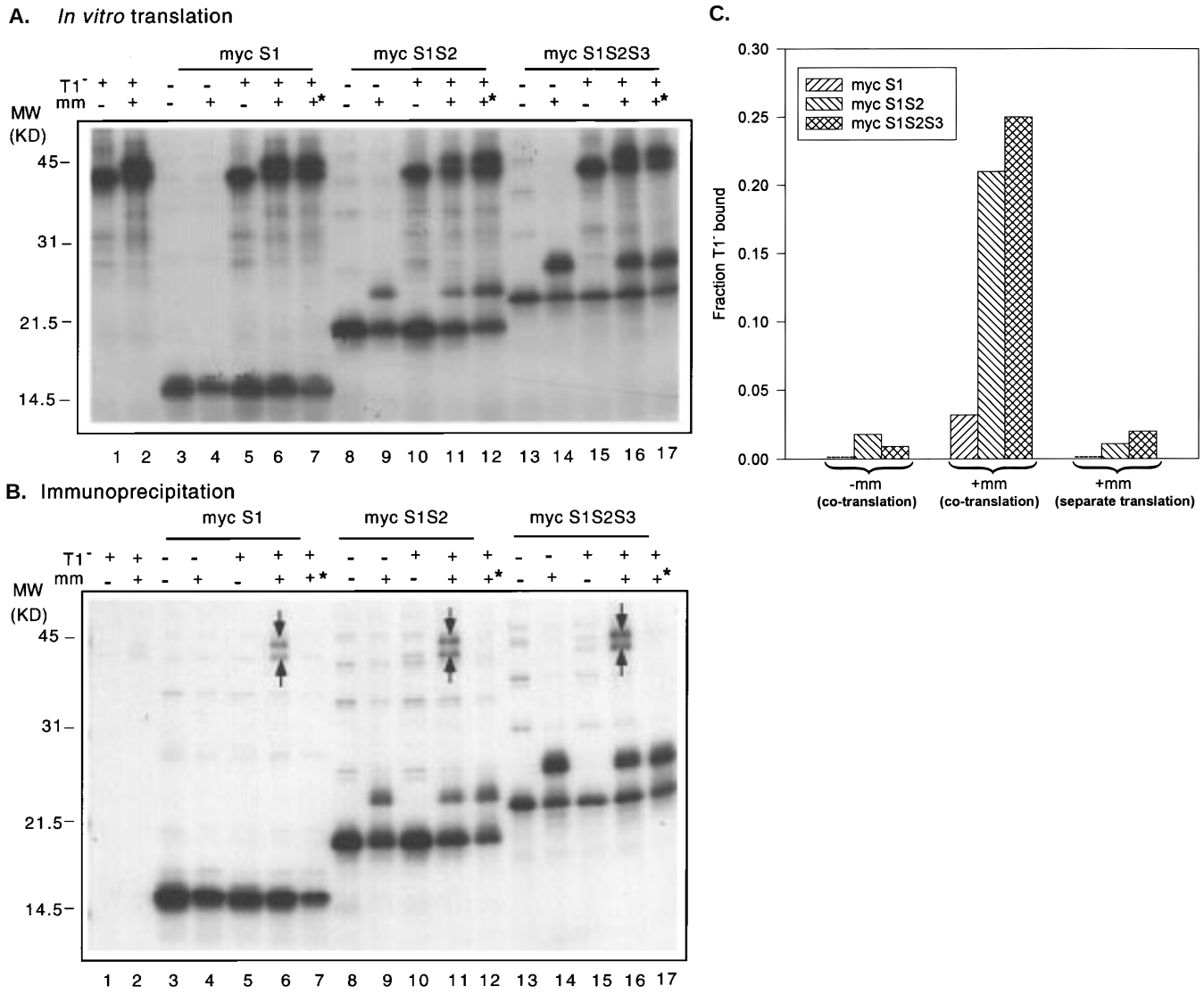

FIGURE 6: Peptide−protein association in the absence and presence of microsomal membranes. (A) myc-S1, myc-S1-S2, and myc-S1-S2-S3 were each translated separately or together with Kv1.3(T1⁻) in the absence or presence of microsomal membranes and run on SDS−PAGE as described in the Methods. (B) Translation mixtures in panel A were immunoprecipitated using anti-myc antibody. For both panels A and B, an asterisk above the lane denotes that the peptide fragment and Kv1.3(T1⁻) were translated separately, and the resulting reaction mixtures were combined and incubated for an additional hour before immunoprecipitation. (C) The fraction of total Kv1.3(T1⁻) bound to peptide fragment was plotted for the data shown in panels A and B.

S1-S2 and myc-S1-S2-S3 associated strongly. The strength of association of Kv1.3(T1⁻) with myc-S1-S2-S3 is greater than that of Kv1.3(T1⁻) with myc-S1, consistent with the greater ability of S1-S2-S3 to suppress Kv1.3 currents. We do not think that the effects of S1-S2-S3 are due to nonspecific effects of three contiguous transmembrane segments because no association of Kv1.3(T1⁻) was observed with two different control membrane proteins containing either one or three transmembrane segments.

The S1-S2 and S1-S2-S3 peptides may represent regions of Kv1.3 that contain inter-subunit association sites. Alternatively, these peptides may represent Kv1.3 regions interacting with an auxiliary protein that binds individual K^+ channel subunits and coordinates the tetramerization of K^+ channel subunits. The first possibility seems plausible because myc-S1-S2-S3 immunoprecipitated with Kv1.3(T1⁻), S2-COOH, S1-S2-S3, and S3-S4-S5 (strong suppressors (*18*)) but not with S5-COOH (data not shown), a peptide fragment that does not suppress Kv1.3(T1⁻) (*18*). The S2-COOH peptide is missing the first 231 amino acids, including the NH_2-terminus, the S1 segment, and most of the S1−S2 loop (*18*). The S5-COOH peptide is missing the first 329 amino acids, including the NH_2-terminus, the S1−S4 segments, and most of the S4−S5 loop (*18*). Based on carbonate extraction assays and N-linked glycosylation, each of these peptide fragments integrates into the membrane (Figure 8, this paper; *18*). On the basis of protease protection assays, the COOH terminus, when present, is located in the cytosol, i.e., the native orientation (data not shown). Thus, the observation that myc-S1-S2-S3 associated with all the test peptides but not with S5-COOH indicates that putative association sites for myc-S1-S2-S3 may reside in transmembrane segments S1−S4. (The lack of effect by S5-COOH may be due to an incorrect topology of the individual transmembrane segments S5 and/or S6 and does not preclude additional association sites in S5-COOH). It is most likely that the region of peptide−peptide association in S1-S2-S3 involves the transmembrane segments because an S1-S2-S3 peptide missing 20 amino acids in the S1−S2 loop also suppressed Kv1.3(T1⁻) equally well (Tu and Deutsch, unpublished data). For this

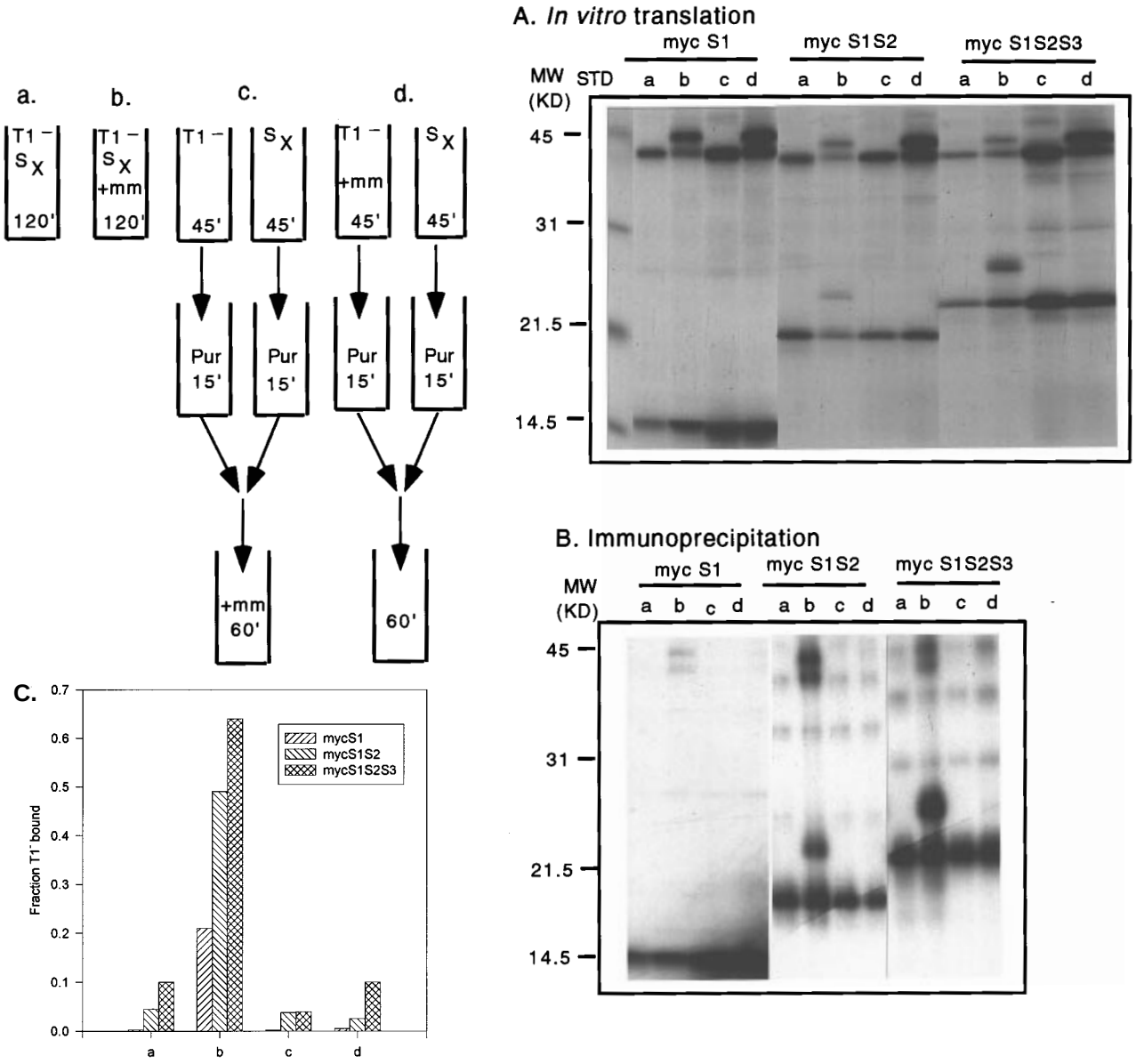

FIGURE 7: Peptide−protein association in posttranslationally mixed reaction products. (A) myc-S1, myc-S1-S2, and myc-S1-S2-S3 were each translated separately or together with Kv1.3(T1$^-$) in the absence or presence of microsomal membranes and run on SDS−PAGE as described in the Methods. Labels a−d above each lane indicate the conditions used for each of the translation steps prior to immunoprecipitation. The presence of microsomal membranes is indicated by mm, and peptide is indicated by S_x. Protocol a means that Kv1.3(T1$^-$) and peptide were translated together without membranes for 2 h; protocol b means that Kv1.3(T1$^-$) and peptide were translated together with membranes for 2 h; protocol c means that Kv1.3(T1$^-$) and peptide were translated separately, each without membranes for 45 min, then puromycin (1 mM) was added to each, incubated for 15 min, followed by combining the two reaction mixtures, adding membranes, and incubating for 60 min; protocol d means that Kv1.3(T1$^-$) was translated with membranes separately from peptide without membranes, each for 45 min, then puromycin was added to each and incubated for 15 min, followed by combining the two reaction mixtures, and incubating for 60 min. All incubations were carried out at 30 °C. (B) Translation mixtures in panel A were immunoprecipitated using anti-myc antibody. (C) The fraction of total Kv1.3(T1$^-$) bound to peptide fragment was plotted for the data shown in panels A and B.

reason, we refer to these putative association sites as IMA (intramembrane association) sites.

Our data support a model in which association of peptide and Kv1.3(T1$^-$) occurs between transmembrane segments in the plane of the lipid bilayer. Although we cannot rule out the possibility that extramembraneous loops also contribute and that the presence of membranes positions these loops appropriately for association interactions to occur. Because these loops are short, it is more likely that transmembrane segments themselves mediate association in the membrane. Three lines of evidence support these possibilities. First, peptide and Kv1.3(T1$^-$) associate efficiently only when the peptide and protein are translated together in the presence of membranes. Second, the time course studies demonstrate that most association (>90%) occurs only after protein synthesis and integration into the membrane are complete. Third, a single transmembrane segment, S1, interacted poorly with Kv1.3(T1$^-$), whereas S1-S2 and S1-S2-S3 interacted strongly with Kv1.3(T1$^-$). S1 did not integrate efficiently into the membrane (<30%); however, S1-S2 and S1-S2-S3 each integrated into the membrane very efficiently (70−90%). Membrane integration can be complex in polytopic proteins, requiring cooperation between multiple transmembrane segments (*22*). Furthermore, integration of polytopic membrane proteins may be delayed until translation terminates and/or the nascent protein detaches

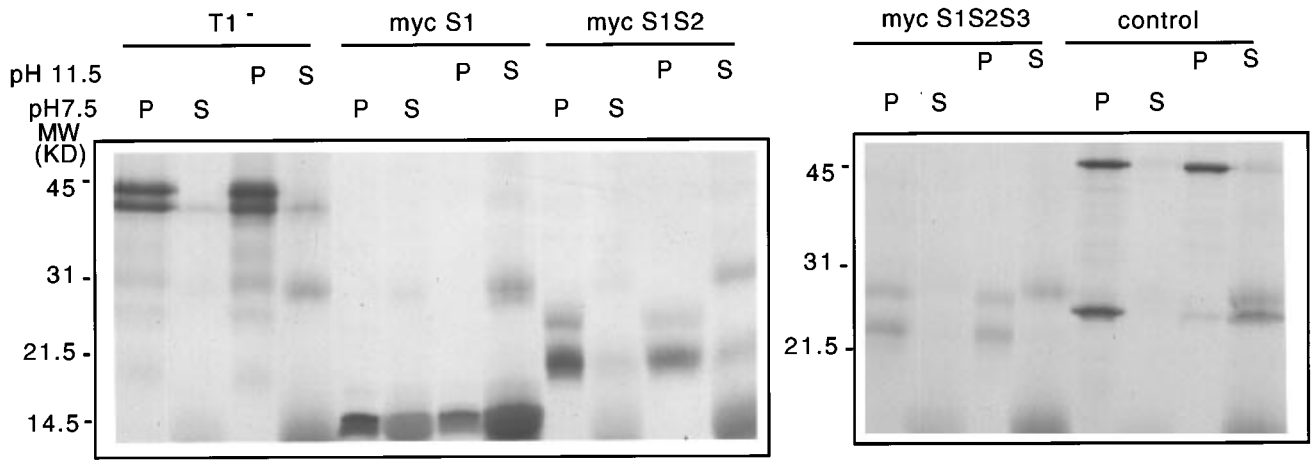

FIGURE 8: Integration of Kv1.3(T1−) peptide fragments into microsomal membranes. Myc-labeled Kv1.3(T1−) and peptide fragments were translated in the presence of microsomal membranes. The translation products were extracted into either Tris buffer (pH 7.5) or carbonate buffer (pH 11.5) and centrifuged to give pellet (P) and supernatant (S) fractions. The pellet contains the membrane fraction of protein. The following control cRNA were simultaneously translated in the assay: S.L.ST.gG.P., which encodes a chimeric integral transmembrane protein (45 kDa) and BPI, which encodes a secreted full-length bovine pre-prolactin protein (25 kDa). The former should remain in the pellet fraction at pH 7.5 and pH 11.5, whereas the latter will be in the pellet (microsome lumen) at pH 7.5 and in the supernatant at pH 11.5.

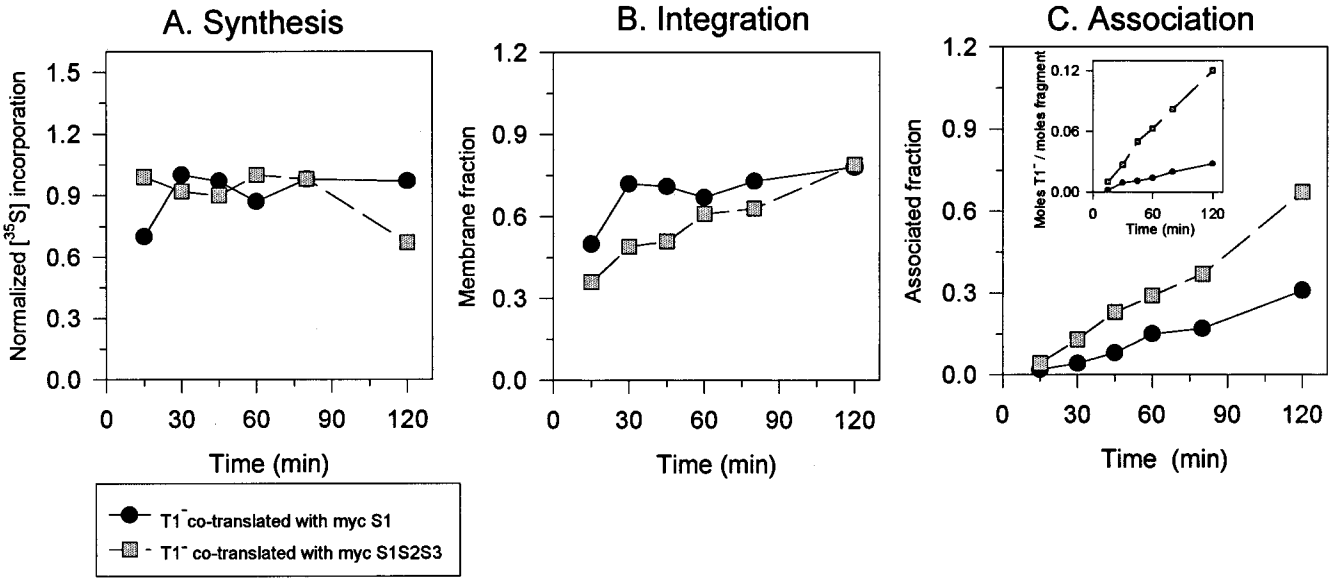

FIGURE 9: Time course of synthesis, membrane integration, and association of Kv1.3(T1−) and peptide fragments. Kv1.3(T1−) was co-translated with myc-labeled S1 or S1-S2-S3 in microsomal membranes and at the indicated times assayed for [35S] incorporation (panel A), distribution into pellet (P) and supernatant (S) fractions in a carbonate extraction assay (panel B), and co-immunoprecipitation of Kv1.3(T1−) by anti-myc antibody (panel C). The ordinate values in panel A were calculated as the ratio of cpm to the maximum cpm for Kv1.3(T1−). The ordinate values in panel B represent the fraction of total Kv1.3(T1−) integrated into the membrane and were calculated as the ratio of pellet cpm to total (pellet + supernatant) cpm. The ordinate values in panel C represent the fraction of total Kv1.3(T1−) associated with peptide fragment and were calculated as the ratio of Kv1.3(T1−) cpm in the immunoprecipitate, corrected for immunoprecipitation efficiency, to the Kv1.3(T1−) cpm in the translation mixture. Panel C (inset): The ordinate values represent the mole ratio of Kv1.3(T1−) to peptide fragment and were calculated as the ratio of Kv1.3(T1−) cpm in the immunoprecipitate to peptide fragment cpm in the immunoprecipitate, each normalized to the number of methionines in the protein. For panels A−C, the average protein concentration for myc-S1 was twice that of myc-S1-S2-S3 to compensate for lower membrane integration of S1 versus S1-S2-S3. Similar results were obtained in two additional, independent experiments.

from the ribosome (*29*). For single spanning proteins, this is proposed to occur in an ordered multistep process in which transmembrane segment(s) pass through discrete states at the multilayered translocon before integration into the bilayer is complete (*30*).

Integration of Kv1.3(T1−) and S1-S2-S3 preceded the rate-limiting association step in oligomerization. This contrasts with the co-translational model proposed by Deal et al. (*31*) for assembly of heterotetramers of full-length Kv1.1 and Kv1.4. However, the latter study did not identify the compartment in which association occurred and only examined full-length protein because their antibody was directed against the C-terminus of Kv1.4. As shown by our experiments, synthesis and integration of Kv1.3(T1−) and S1-S2-S3 are so rapid that, under normal translation conditions, they appear synchronous. This may explain the results of Deal et al. Alternatively, we cannot rule out the possibility that cytoplasmic NH_2-terminal recognition motifs may alter the temporal and spatial relationships between synthesis, integration, and association of K^+ channel proteins. However, in the absence of an NH_2-terminal T1 domain, protein−protein interaction is the rate-determining, membrane-

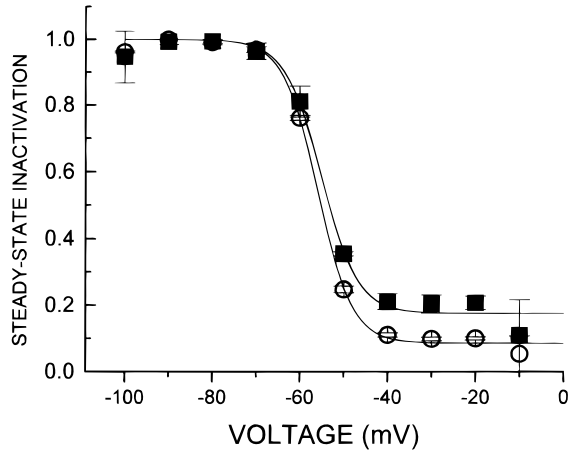

FIGURE 10: Steady-state inactivation versus voltage of Kv1.3($T1^-$) expressed in oocytes. Kv1.3($T1^-$) cRNA was co-injected with either S1 (circle) or S1-S2-S3 (square) in a 1:2 mole ratio into oocytes and recorded 48 h postinjection. Peak current was measured during a 45-ms depolarization to +50 mV after a 2.5-s period at the indicated negative voltages, followed by a 0.1 ms step to −100 mV. Between stimuli, oocytes were held at −100 mV for 50 s. Data represent mean ± SEM for three cells.

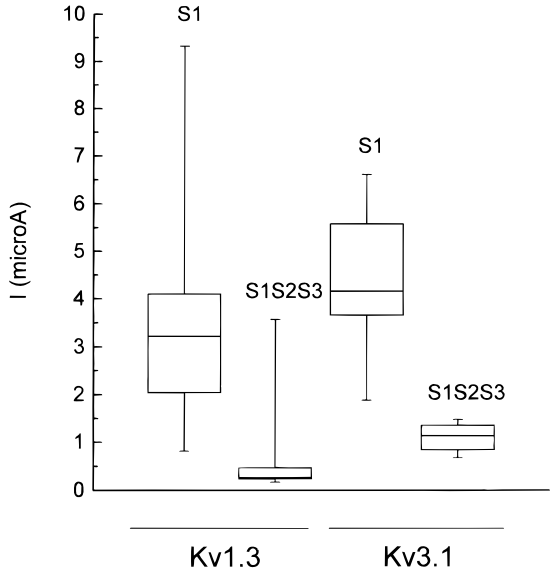

FIGURE 11: Effect of truncated Kv1.3 (S1-S2-S3) on full-length Kv1.3 and Kv3.1 current in oocytes. Oocytes were co-injected with cRNA for Kv1.3 and either S1 (control) or S1-S2-S3 and with cRNA for Kv3.1 and either S1 or S1-S2-S3 (in a 1:2 mole ratio). Recordings were made 20 h postinjection. Peak current at +50 mV was measured. Data are represented as box plots ($n = 11$, Kv1.3; $n = 8$, Kv3.1). In both cases, current in the presence of S1-S2-S3 was significantly less than control, with $p < 0.001$, as determined from a nonparametric Mann−Whitney rank sum test. The bath Ringer solution contained (in mM): 116 NaCl, 2 KCl, 1.8 $CaCl_2$, 2 $MgCl_2$, 5 Hepes (pH 7.6). The holding potential was −100 mV.

delimited step in association. Our findings support a model in which the endoplasmic reticulum membrane itself facilitates K^+ channel tetramerization even when subunits are expressed at low levels, thus permitting efficient and rapid oligomerization relative to non-membrane assembly compartments (*26*).

We also propose that the S1-S2-S3 region of Kv1.3 may serve a specific role in channel formation. The potent suppression of full-length Kv1.3 by S1-S2-S3 suggests that these transmembrane segments contain intersubunit association sites used in K^+ channel assembly. These sites are conserved across the subfamilies of voltage-gated K^+ channels and may contribute to assembly of other subfamily isoforms. For instance, S1-S2-S3 derived from Kv1.3 suppressed both full-length Kv1.3 and Kv3.1 by ∼80%. Moreover, these full-length channels contain cytoplasmic T1 domains (*5*, *17*), and yet their suppression by S1-S2-S3 suggests that, even when putative T1 interactions occur in the aqueous phase, interactions between IMA sites on channel proteins must still occur in the lipid bilayer. The relative contributions of T1 and IMA interactions to specificity and stabilization is likely to depend on the isoform and subfamily.

ACKNOWLEDGMENT

We thank Dr. David Andrews (McMaster University, Ontario, Canada) for helpful discussions and for supplying us with microsomal membranes; Dr. Carolyn Mackamer (The Johns Hopkins University, Baltimore, MD) for giving us the coronavirus clone, IBV M; Jianli Lu for assisting in some of the experiments; and Drs. Li Wei Tu and Spike Horn for careful reading of the manuscript.

REFERENCES

1. Hurtley, S. M., and Helenius, A. (1989) *Ann. Rev. Cell Biol. 5*, 277−307.
2. Chothia, C., and Janin, J. (1975) *Nature 256*, 705−708.
3. Popot, J.-L., and Engelman, D. M. (1990) *Bichemistry 29*, 4031−4036.
4. Verrall, S., and Hall, Z. W. (1992) *Cell 68*, 23−31.
5. Li, M., Jan, Y. N., and Jan, L. Y. (1992) *Science 257*, 1225−1230.
6. Shen, N. V., Chen, X., Boyer, M. M., and Pfaffinger, P. (1993) *Neuron 11*, 67−76.
7. Babila, T., Moscucci, A., Wang, H., Weaver, F. E., and Koren, G. (1994) *Neuron 12*, 615−626.
8. Lemmon, M. A., Flanagan, J. M., Hunt, J. F., Adair, B. D., Bormann, B.-J., Dempsey, C. E., and Engelman, D. M. (1992) *J. Cell Biol. 267*, 7683−7689.
9. Lemmon, M. A., Flanagan, J. M., Treutlein, H. R., Zhang, J., and Engelman, D. M. (1992) *Biochemistry 31*, 12719−12725.
10. Cosson, P., and Bonafacino, J. S. (1992) *Science 258*, 659−662.
11. Manolios, N., Bonifacino, J. S., and Klausner, R. D. (1990) *Science 249*, 274−277.
12. Cosson, P., Lankford, S. P., Bonifacino, J. S., and Klausner, R. D. (1991) *Nature 351*, 414−416.
13. Matteson, D. R., and Deutsch, C. (1984) *Nature 307*, 468−471.
14. DeCoursey, T. E., Chandy, K. G., Gupta, S., and Cahalan, M. D. (1984) *Nature 307*, 465−468.
15. Panyi, G., and Deutsch, C. (1996) *J. Gen. Physiol. 107*, 409−420.
16. Shen, N. V., and Pfaffinger, P. J. (1995) *Neuron 14*, 625−633.
17. Xu, J., Yu, W., Jan, Y.-N., Jan, L.-Y., and Li, M. (1995) *J. Biol. Chem. 270*, 24761−24768.
18. Tu, L., Santarelli, V., Sheng, Z.-F., Skach, W., Pain, D., and Deutsch, C. (1996) *J. Biol. Chem. 271*, 18904−18911.
19. Rosenberg, R. L., and East, J. E. (1992) *Nature 360*, 166−169.
20. Chahine, M., Chen, L., Barchi, R. L., Kallen, R. G., and Horn, R. (1992) *J. Mol. Cell Cardiol. 24*, 1231−1236.
21. Tu, L., Santarelli, V., and Deutsch, C. (1995) *Biophys. J. 68*, 147−156.
22. Skach, W., and Lingappa, V. R. (1993) *J. Biol. Chem. 268*, 23552−23561.
23. Machamer, C. E., and Rose, J. K. (1987) *J. Cell Biol. 105*, 1205−1214.

24. Evan, G., Lewis, G., Ramsay, G., and Bishop, M. J. (1985) *Mol. Cell Biol. 5*, 3610−3616.
25. MacKinnon, R. (1991) *Nature 350*, 232−235.
26. Helenius, A., Marquardt, T., and Braakman, I. (1992) *Trends Cell Biol. 2*, 227−231.
27. Spencer, R., Sokolov, Y., Li, H., Takenaka, B., Milici, A. J., Aiyar, J., Nguyen, A., Park, H., Jap, B. K., Hall, J. E., and Chandy, K. G. (1997) *J. Biol. Chem. 272*, 2389−2395.
28. Heginbotham, L., Odessey, E., and Miller, C. (1997) *Biochemistry 36*, 10335−10342.
29. Borel, A. C., and Simon, S. M. (1996) *Cell 35*, 379−389.
30. Do, H., Falcone, D., Lin, J., Andrews, D. W., and Johnson, A. E. (1996) *Cell 85*, 369−378.
31. Deal, K. K., Lovinger, D. M., and Tamkun, M. M. (1994) *J. Neurosci. 14*, 1666−1676.

BI971490J